Communication

Influence of Extreme Thermodynamic Conditions and Pyrite Surfaces on Peptide Synthesis in Aqueous Media

Eduard Schreiner, Nisanth N. Nair, and Dominik Marx

J. Am. Chem. Soc., **2008**, 130 (9), 2768-2770 • DOI: 10.1021/ja7108085

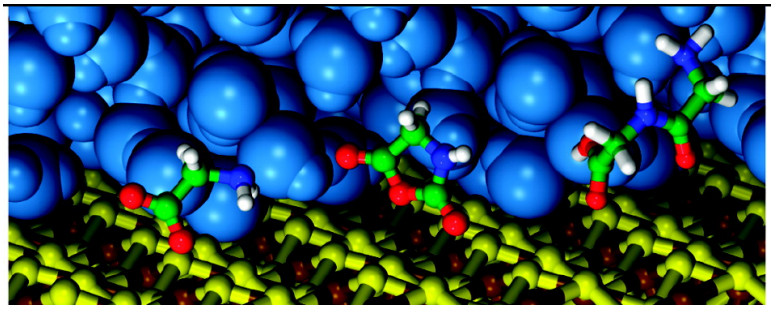

J|A|C|S
COMMUNICATIONS

Published on Web 02/07/2008

Influence of Extreme Thermodynamic Conditions and Pyrite Surfaces on Peptide Synthesis in Aqueous Media

Eduard Schreiner,* Nisanth N. Nair, and Dominik Marx

Lehrstuhl für Theoretische Chemie, Ruhr-Universität Bochum, 44780 Bochum, Germany

Received December 4, 2007; E-mail: eduard.schreiner@theochem.rub.de

Understanding reaction mechanisms, free energetics, and kinetics of complex chemical reactions in the liquid state, in particular in water, is a challenge to computer simulation. Although impressive progress has been achieved in recent years,[1] the efficient synthesis of peptides in water remains largely elusive. A crucial ingredient of peptidization in aqueous environments is certainly the suitable activation of amino acids, thus allowing for elongation or copolymerization steps to occur. A promising route among others is their activation in the form of cyclic α-amino acid *N*-carboxyanhydrides (NCAs or Leuchs anhydrides),[2] which opens up efficient polymerization pathways. Chemically, NCAs offer the advantage of an activated CO group while simultaneously protecting the amino group. In addition, unlike in organic solvents with high nucleophilicity and donor ability such as *N*,*N*-dimethylformamide (DMF), *N*-methylpyrrolidone (NMP), dimethyl sulfoxide (DMSO),[3] or pyridine,[4] polymerization of NCAs in bulk water yields *linear* polypeptides.[2]

Along these lines, it has been suggested that NCAs themselves can be obtained from thiocarbamates via carbonyl sulfide (COS) addition to an amino acid. Although the yield of peptides along the COS activation route is quite low in water, salts of heavy metals and alkylating or oxidizing agents can increase the yield considerably.[5,6] It has been speculated that such an activation of amino acids might be relevant for prebiotic peptide synthesis.[2,7] However, mechanistic insights[2] into the formation of NCAs from amino acids and COS are limited to early speculations in footnote 16 of ref 8 and some evidence for the presence of an isocyanate species.[6]

Furthermore, it has been speculated that extreme temperature and pressure conditions might facilitate the formation of oligopeptides along this NCA pathway.[5,9] This idea is supported by the observation that the *neutral* form of amino acids and peptides is required, which could be stabilized in hot-pressurized water.[10] In this context, it must be appreciated that the dielectric constant of water at its critical point (where $T_c = 647.1$ K and $p_c = 22.1$ MPa) is dramatically reduced to only about 6 (instead of ∼80 at ambient conditions), thus stabilizing neutral reactants and intermediates with respect to charged or zwitterionic ones.[10] Chemically speaking, water at such extreme conditions is indeed a different substance, which implies that well-known concepts from organic chemistry might be misleading rather than helpful here.[10] Finally, it has been suggested that also mineral surfaces,[11] in particular pyrite, could be a useful additional ingredient not only to bring reactants together but also to allow for heterogeneous catalytic effects.[5] Still, the key step of "The formation of NCAs according to Scheme 39 [Scheme 39: Formation of NCAs through activation of amino acids by COS.] is still hypothetical and needs experimental verification" (cited from section 10 of ref 2), even at ambient conditions in bulk water.

In the following, we investigate peptide synthesis in various aqueous environments, which provides detailed insights into the free energy profiles and pathways which are at the heart of amino acid activation via NCAs and subsequent elongation. In particular, we use the recently introduced combination[12] of the metadynamics sampling technique[13] with Car−Parrinello *ab initio* simulations.[14,15] Whereas the latter allows one to take the electronic structure in condensed matter molecular dynamics simulations into account and thus to access chemical transformations, the former permits the exploration of complex rare events such as chemical reactions subject to large free energy barriers and high-dimensional reaction coordinates.[16] The electronic structure was described within Kohn−Sham density functional theory in its plane wave/pseudopotential formulation[15] using the PBE[17] exchange-correlation functional, which has been shown to perform well for the system of interest[18−20] (see also Supporting Information, SI).

In computer simulations, the full reaction coordinate space must be spanned approximately by a subset of most relevant generalized coordinates. In all reaction steps investigated here, either two- or three-dimensional reaction subspaces were defined (as specified in SI Table 2). In addition to using interatomic distances between *two specified* reacting sites, the more general coordination numbers[21] are utilized. Coordination numbers can be defined between *two classes* of atomic species that can contain all atoms of a given type in the system, which thus greatly increases the effective dimensionality of the sampled reaction subspace by not selecting *a priori* the individual reacting atoms. To aid clarification in this presentation, all pertinent methodological and technical details are collected in the SI.

At the core of this study is the formation of a peptide bond between two glycine molecules, which were chosen as the computationally most convenient amino acid in addition to having been studied earlier in ref 5 in the framework of interest, at three vastly different reaction conditions: ambient bulk water at about 300 K and 0.1 MPa (ABW), hot-pressurized bulk water at about 500 K and 20 MPa (HPW), and hot-pressurized water at the pyrite interface (PIW) on the (001) face of FeS_2 according to refs 18−20.

The multitude of results can be condensed into the peptide synthesis cycle depicted in Figure 1. The first important observation is that the *neutral* form of glycine **2**, and thus step A in Figure 1, is necessary for its activation by COS to yield thiocarbamate **3** in step B. As evidenced by the computed free energy barriers (reported in units of k_BT to allow their convenient comparison at two different temperatures), HPW extreme conditions stabilize the required neutral form **2**, consistent with the lowering of the dielectric constant of HPW, whereas in ABW species **2** is found to convert to the zwitterion **1** on a time scale as fast as ∼1 ps. Interestingly, alkaline pH has been used in the experiments on COS-activated prebiotic synthesis of peptides[6] *at ambient reaction conditions*, which induces a similar shift of the amino acid equilibrium toward the neutral form.

Second, the formation of thiocarbamate **3** is strongly enhanced when going from ambient (ABW, 36 k_BT_{300}) to extreme conditions (HPW, 20 k_BT_{500}). Mechanistically, in both ABW and HPW, the

 10.1021/ja7108085 CCC: $40.75

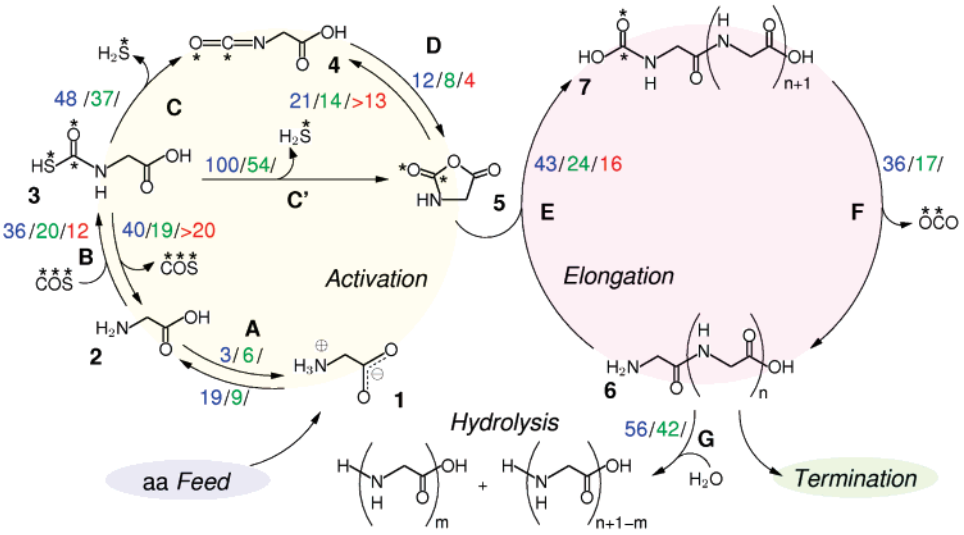

Figure 1. The investigated peptide synthesis cycle, comprising amino acid input, amino acid activation, peptidization leading to elongation, and termination as well as possible destructive hydrolysis of the peptide; see text for discussion. The atoms of the activating COS molecule are marked by stars throughout the entire cycle. The calculated free energy barriers (reported in units of k_BT) for the three conditions considered are color coded and given in the sequence ambient bulk water, ABW (blue)/hot-pressurized water, HPW (green)/pyrite interfacial water, PIW (red).

first step in process B is the addition of the nitrogen of the amino group to the carbon of the COS molecule, resulting in a charged intermediate which further deprotonates, mediated by a solvent water molecule, to form thiocarbamate **3**. Overall, due to the influence of HPW conditions, the effective forward barrier is reduced by a factor of 2. When occurring on the ideal mineral surface, this barrier is lowered by another factor of 2 (PIW, 12 k_BT_{500}).

Even though pyrite sulfur atoms take over the role of proton acceptors (from water molecules in ABW and HPW) at these PIW conditions, the essential heterogeneous catalytic effect can be traced back to the reduction of the entropic contribution to the rate-determining barrier. This is achieved by immobilizing the reactants, thereby minimizing fluctuations, which is genuinely a geometric effect when reaction environments are reduced from three to two dimensions. Note that, although fast desorption is likely to occur on ideal surfaces,[18] such effects will be efficacious in the presence of ubiquitous surface defects that prolong retention times by several orders of magnitude, e.g., in the case of sulfur vacancies[19] (*vide infra*, step **C**′′′′).

The next step, formation of NCA **5**, is believed to be rate-limiting and thus most crucial for a productive peptide synthesis cycle.[6] Despite early speculations mentioned in a footnote,[8] the mechanism for this most important process remains unknown.[2,6] The first possibility investigated is the direct cyclization (**C**′) of thiocarbamate **3** to NCA **5**, involving breakage of the C−S bond and elimination of an SH^- anion. Again, HPW strongly favors the formation of this reactive intermediate when compared to ABW by halving the effective barrier from 100 k_BT_{300} to 54 k_BT_{500}. However, even in HPW, the reaction barrier for the formation of this key intermediate **5** remains substantial. Surprisingly, once the NCA was synthesized via this direct route, the simulations produced a ring-opening side reaction that resulted in an isocyanate structure **4** (see SI for details), the presence of which has been suggested experimentally.[6] This encouraged us to carefully investigate an indirect route, i.e., thiocarbamate → isocyanate → NCA, according to paths **C** and **D**. Most importantly, the data clearly show (see Figure 1) that both barriers involved are much lower than in the direct route **C**′, thus strongly supporting mechanistic speculations that involve such isocyanate species.[6,8] Moreover, HPW extreme conditions favor both

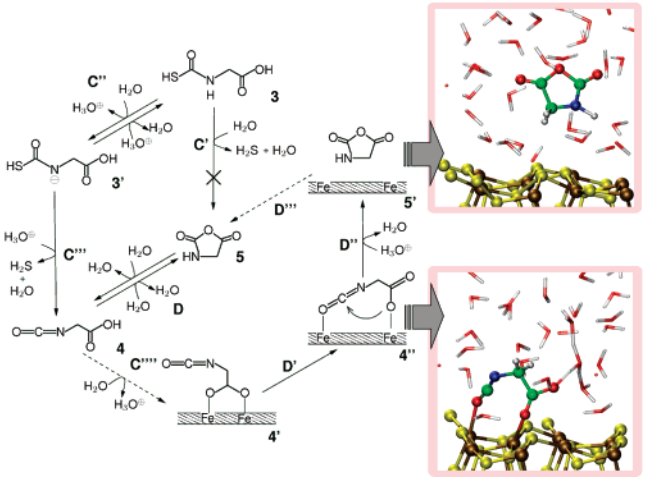

Figure 2. Mechanism of the formation of NCA **5** from thiocarbamate **3**. Thin solid arrows show the reaction pathways as obtained from explicit simulations, while the dashed lines indicate the transfer of molecules between bulk and surface; the crossed direct formation path **C**′ is very unlikely in view of its high activation free energy (see Figure 1). Snapshots of two representative configurations sampled from simulations at the pyrite−water interface demonstrate scaffolding in terms of preformation of the cyclic topology of NCA upon bidentate chemisorption: hydrogen, white; oxygen, red; carbon, green; nitrogen, blue; sulfur, yellow; iron, brown.

reactions like in the previous steps **A** and **B**. Finally, the formation of isocyanate **4** from thiocarbamate **3** is identified to be indeed the rate-limiting step of the entire peptide synthesis cycle.

From the mechanism dissected in Figure 2, it is evident that the formation of isocyanate **4** is a two-step process, in which first **3** deprotonates at the nitrogen (**C**′′), followed by an elimination of the SH^- anion (**C**′′′), which readily converts to H_2S. Both steps are associated with high activation energies, the latter being rate-determining. Elimination of SH^- is expected to be the bottleneck because of the poor leaving nature of this group, which is underpinned by the noticeable catalytic effect of alkylating and oxidizing agents.[6]

In order to investigate possible surface effects on the formation of NCA, we attached in step **C**′′′′ the deprotonated isocyanate **4** near a sulfur vacancy defect on pyrite;[19] we did not observe any

chemical participation of this defect, but sulfur vacancies are useful to increase retention times of reactive species on pyrite surfaces.[19] During the simulation, the isocyanate oxygen of **4′** strongly attaches to an iron atom to yield **4″** at the expense of detaching one of the two carboxylate oxygens (**D′**), which expedites greatly the cyclization **D″** together with the protonation of nitrogen in a concerted fashion. Clearly, the bidentate initial chemisorption of **4′**, which easily gives rise to **4″**, preforms a cyclic structure that tremendously facilitates formation of the cyclic topology of adsorbed NCA **5′**, which readily desorbs to **5** at PIW conditions (**D‴**). This scaffolding effect due to the surface, which is very distinct from the entropic effect observed earlier, is responsible for lowering the effective reaction barrier of this step by a factor of 2 in comparison to HPW.

At this stage, having synthesized an activated amino acid in form of NCA **5** with the help of COS, peptidization **E** and thus elongation can take place. Note that, once again, the amino acid (or newly formed peptide if $n \geq 1$ in Figure 1) prefers to react with NCA **5** in its neutral form **6**, which is favored by extreme conditions, and that the effective relative activation barrier for this reaction is considerably lower in HPW as well (HPW, 24 k_BT_{500} versus ABW, 43 k_BT_{300}). The main contribution to this acceleration is due to the high temperature, even though slightly different mechanisms are observed: HPW prefers adduct formation in concert with ring opening, whereas ABW stabilizes several charged intermediates and thus favors a stepwise peptide bond formation. On the ideal surface, the free energy barrier for peptidization **E** is furthermore found to be reduced significantly from 24 k_BT_{500} in HPW to only 16 k_BT_{500} at PIW conditions, which is again largely an entropic effect (note that using a defective surface is expected to increase the retention time sufficiently[19]). Also, in the final decarboxylation step **F**, HPW is found to reduce the effective barrier dramatically from 36 k_BT_{300} in ABW to only 17 k_BT_{500}. In both HPW and ABW, the protonation at the nitrogen by a water molecule is the initial step, succeeded by the release of CO_2, yielding peptide **6**, which is the final target.

In linking all reaction steps, a complete peptide synthesis cycle consisting of activation and elongation steps has been described in mechanistic detail which is clearly shown to be favored by both a high-temperature/high-pressure reaction environment and the presence of a pyrite surface. Still, an important aspect that remains to be scrutinized is the efficiency of peptide hydrolysis in relation to peptide formation. It is found that the effective barrier of this decisive reverse reaction **G** of peptide synthesis (HPW, 42 k_BT_{500}; ABW, 56 k_BT_{300}) is higher than any forward barrier to peptide formation, thus suggesting net peptide accumulation for the proposed synthesis mechanism.

To summarize, the simulations delineate pathways connecting the crucial activation and elongation steps through which peptides can be produced out of amino acids and COS via an indirect isocyanate/NCA route. In addition, the roles played by the extreme thermodynamic conditions and the pyrite mineral surfaces have been assessed and quantified. The rate-determining step of the constructive branch of the cycle is the activation of amino acids to NCA via an isocyanate intermediate. This indirect route is shown to be clearly preferred over the direct cyclization of thiocarbamate. Importantly, the simulations reveal how hot-pressurized water conditions alter the relative stability of reactants, transition states, intermediates, and products, thus favoring peptide production by appropriately influencing individual reaction steps in this cycle. Furthermore, pyrite surfaces were found to act as catalysts and additionally as a support, thus leading to remarkable reductions of free energy barriers by scaffolding and/or immobilization of reactants. In addition to their chemical relevance, these results might be useful in the framework of prebiotic peptide synthesis.[5,6]

Acknowledgment. Partial financial support was provided by Deutsche Forschungsgemeinschaft (DFG Normalverfahren MA 1547/7) and by Fonds der Chemischen Industrie (FCI). The simulations were carried out on the IBM Blue Gene system at John von Neumann Institute for Computing (NIC) at Forschungszentrum Jülich (Germany).

Supporting Information Available: Description of the system setup, theoretical background on ab initio metadynamics, simulation parameters and protocols, and assessment of accuracy. This material is available free of charge via the Internet at http://pubs.acs.org.

References

(1) (a) Curioni, A.; Sprik, M.; Andreoni, W.; Schiffer, H.; Hutter, J.; Parrinello, M. *J. Am. Chem. Soc.* **1997**, *119*, 7218−7229. (b) Meijer, E. J.; Sprik, M. *J. Am. Chem. Soc.* **1998**, *120*, 6345−6355. (c) Ensing, B.; Buda, F.; Blöchl, P.; Baerends, E. J. *Angew. Chem., Int. Ed.* **2001**, *40*, 2893−2895. (d) Stubbs, J. M.; Marx, D. *J. Am. Chem. Soc.* **2003**, *125*, 10960−10962. (e) Boero, M.; Ikeshoji, T.; Liew, C. C.; Terakura, K.; Parrinello, M. *J. Am. Chem. Soc.* **2004**, *126*, 6280−6286. (f) Ensing, B.; Klein, M. L. *Proc. Natl. Acad. Sci.* **2005**, *102*, 6755−6759. (g) Handgraaf, J. W.; Meijer, E. J. *J. Am. Chem. Soc.* **2007**, *129*, 3099−3103.
(2) Kricheldorf, H. R. *Angew. Chem., Int. Ed.* **2006**, *45*, 5752−5784.
(3) Kricheldorf, H. R.; von Lossow, C.; Schwarz, G. *Macromolecules* **2005**, *38*, 5513−5518.
(4) (a) Bilek, L.; Derkosch, J.; Michl, H.; Wessely, F. *Monatsh. Chemie/Chemical Monthly* **1953**, *84*, 717−740. (b) Kricheldorf, H. R.; von Lossow, C.; Schwarz, G. *J. Polym. Sci. Part A: Polym. Chem.* **2006**, *44*, 4680−4695.
(5) Huber, C.; Wächtershäuser, G. *Science* **1998**, *281*, 670−672.
(6) Leman, L.; Orgel, L.; Ghadiri, M. R. *Science* **2004**, *306*, 283−286.
(7) Pascal, R.; Boiteau, L.; Commeyras, A. *Top. Curr. Chem.* **2005**, *259*, 69−122.
(8) Deweye, R. S.; Schoenewald, F.; Joshua, H.; Paleveda, W.; Schwam, H.; Barkemeyer, H.; Arison, B. H.; Veber, D. F.; Strachan, R. G.; Milkowski, J.; Denkewaltear, R. G.; Hirschmann, R. *J. Org. Chem.* **1971**, **36**, 49−59.
(9) Wächtershäuser, G. *Phil. Trans. R. Soc. London B* **2006**, *361*, 1787−1808.
(10) Weingärtner, H.; Frank, E. U. *Angew. Chem., Int. Ed.* **2005**, *44*, 2672−2692.
(11) Rimola, A.; Sodupe, M.; Ugliengo, P. *J. Am. Chem. Soc.* **2007**, *129*, 8333−8344.
(12) Iannuzzi, M.; Laio, A.; Parrinello, M. *Phys. Rev. Lett.* **2003**, *90*, 238302-1-4.
(13) Laio, A.; Parrinello, M. *Proc. Natl. Acad. Sci.* **2002**, *99*, 12562−12566.
(14) Car, R.; Parrinello, M. *Phys. Rev. Lett.* **1985**, *55*, 2471−2474.
(15) Marx, D.; Hutter, J. In *Modern Methods and Algorithms of Quantum Chemistry*; NIC: FZ Jülich, 2000. For downloads see http://www-.theochem.rub.de/go/cprev.html.
(16) Ensing, B.; De Vivo, M.; Liu, Z.; Moore, P.; Klein, M. L. *Acc. Chem. Res.* **2006**, *39*, 73−81.
(17) Perdew, J. P.; Burke, K.; Ernzerhof, M. *Phys. Rev. Lett.* **1996**, *77*, 3865−3868; *Phys. Rev. Lett.* **1997**, *78*, 1396−31396.
(18) Boehme, C.; Marx, D. *J. Am. Chem. Soc.* **2003**, *125*, 13362−13363.
(19) Nair, N. N.; Schreiner, E.; Marx, D. *J. Am. Chem. Soc.* **2006**, *128*, 13815−13826.
(20) Pollet, R.; Boehme, C.; Marx, D. *Origins Life Evol. Biospheres* **2006**, *36*, 363−379.
(21) Sprik, M. *Chem. Phys.* **2000**, *258*, 139−150.

JA7108085